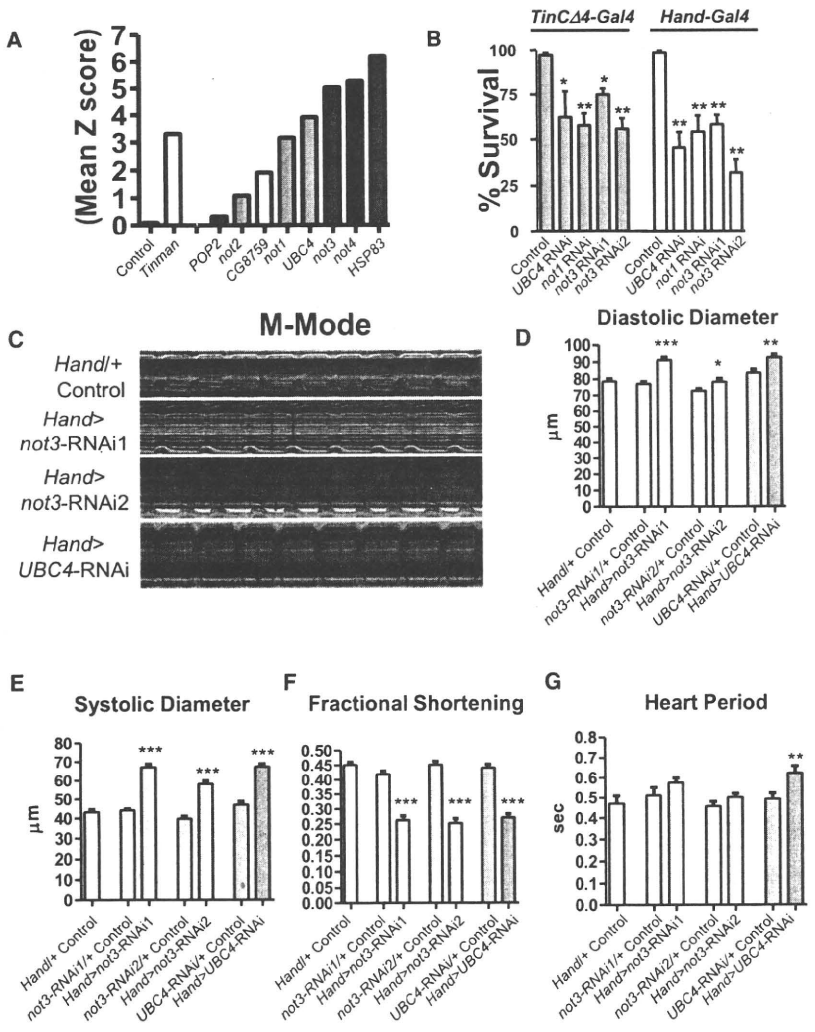


**Figure 3. The CCR4-Not Complex Is a Central Regulator of Adult Heart Function, and Loss of not3 Results in Dilated Cardiomyopathy in *Drosophila***

(A) Mean Z scores for *TinCΔ4-Gal4* x *UAS*-RNAi lines targeting the indicated members of the fly CCR4-Not complex. A negative control ($w^{1118}$ [isogenic to the RNAi library] X *TinΔ4-Gal4*) and the positive control *Tinman* RNAi line are shown.

(B) *not1*, *not3*, and *UBC4* are essential for proper adult heart function in both *Tinman*- and *Hand*-expressing cells. Data are shown as mean ± SEM for at least three replicates. RNAi1 and RNAi2 indicate different transgenic hairpins targeting *not3* . *$p < 0.05$, **$p < 0.01$ by ANOVA.

(C) One-week-old adult flies with *Hand-Gal4* driving *not3* or *UBC4* cardiac-specific knockdown exhibit impaired heart function. M modes provide traces of the heart contractions to document the movements in a 1 pixel wide region of the heart tube over time. *HandG4/+* control are the progeny of *Hand-Gal4* crossed to $w^{1118}$. *Hand>Not3* complex flies are the progeny of *Hand-Gal4* crossed to either *UAS-not3*-RNAi (−1 or −2) or to UAS-*UBC4*-RNAi lines. Fly heart analysis was performed with a MatLab-based image analysis program (Fink et al., 2009; Ocorr et al., 2007b). M modes of the RNAi knockdown hearts reveal dilated diastolic and systolic diameters (double-headed red arrows) and reduced shortening properties (difference between diameters) when compared to M modes of control hearts. Each trace represents a 5 s recording.

(D–G) *Not3* or *UBC4* heart-specific knockdown perturbs several indices of cardiac performance. Progeny of *Hand-Gal4* crossed to two different *UAS-not3*-RNAi lines or an *UAS-UBC4*-RNAi line (experimental) and $w^{1118}$ crossed to *UAS*-RNAi or *Hand-Gal4* driver (controls) were used for these experiments as in (C). *not3* and *UBC4* knockdown led to significantly wider diastolic (D) and systolic (E) diameters, and as a result significantly depressed (F) fractional shortening in all experimental lines relative to controls. *not3* knockdown trended toward a slight lengthening in the heart period (time between consecutive diastolic intervals), while *UBC4* knockdown led to a significant increase in heart period (G). Mean values ± SEM are shown for each group (n = 29–40). Unpaired t tests were performed between each *Hand-Gal4>UAS*-RNAi and each corresponding *UAS*-RNAi/+ control (progeny of $w^{1118}$ crossed to *UAS*-RNAi line). Additionally, one-way ANOVAs with Bonferroni multiple comparison tests revealed no significant differences between the *HandG4/+* control and all *UAS*-RNAi/+ control lines, for any cardiac parameter measured.

*$p < 0.05$, **$p < 0.01$, ***$p < 0.001$. See also Figure S3 and Movie S1.

have not yet been associated with cardiovascular function. We therefore retested components of this pathway using *TinCΔ4-Gal4*-driven knockdown in the heart, which confirmed the phenotype (Figure 3B). Moreover, use of a second heart driver, *Hand-Gal4*, which is expressed with high specificity in myocardial and pericardial cells throughout development and in the adult fly heart (Han and Olson, 2005), showed that silencing of *not1*, *not3*, and *UBC4* resulted in early death when adult flies were shifted to 29°C (Figure 3B).

Since *not3* RNAi gave a strong phenotype with two different *UAS*-RNAi lines (Figure 3B), we focused on the CCR4-Not component *not3*. Cardiac-specific knockdown of *not3* with two different RNAi lines (*Hand>not3*-RNAi: progeny from *Hand*-Gal4 crossed to *UAS-not3*-RNAi) significantly increased both diastolic and systolic diameters and resulted in reduced systolic fractional shortening relative to control flies (Figures 3C–3F and Movie S1). Hearts with cardiac *not3* knockdown also showed slight increases in heart periods (Figure 3G); however, this was not statistically significant. Fluorescent microscopy revealed that *not3* RNAi lines exhibit marked myofibrillar disarray, especially in the conical chamber (Figures 4A–4D). Heart-restricted *not3*-RNAi-mediated knockdown was confirmed by qRT-PCR (Figure S3). In addition, we observed transcriptional downregulation of the Sarcoplasmic/endoplasmic reticulum calcium ATPase

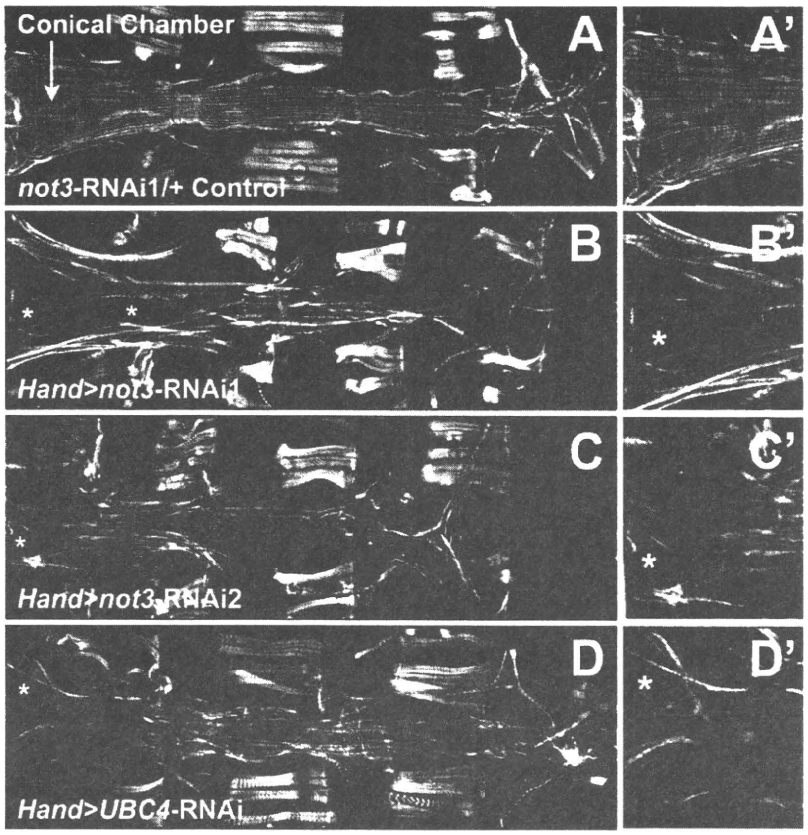


**Figure 4. *not3* and *UBC4* Cardiac-Specific RNAi Knockdown Substantially Perturb Myofibrillar Organization and Content**

(A) Alexa584-phalloidin staining of control *Drosophila* cardiac tubes reveals typical spiraling myofibrillar arrangements within the cardiomyocytes. The fibers, especially those in the conical chamber, located anteriorly, are densely packed with F-actin.

(B–D) Relative to control hearts, *not3* or *UBC4* RNAi knockdown severely disrupts myofibrillar organization and leads to an apparent loss of myofilaments as noted by large gaps in F-actin staining (*) as well as by a lack of myosin heavy chain transcripts (Figure S3F).

(A'–D') Enlarged images of the conical chambers from (A)–(D), respectively, which illustrate the high degree of myofibrillar disarray and large gaps in F-actin staining within the cardiomyocytes of *not3* and *UBC4* RNAi knockdown hearts. Original images were taken at 10× magnification with a Zeiss Imager Z1 fluorescent microscope.

(*Serca2a*, *ATP2A2*), myosin heavy chain (*mhc*, *MYH7*), and the potassium channel *KCNQ* (*kcnq1*, *KCNQ1*) (Figure S3) involved in heart rhythm control. Cardiac-specific knockdown of *not3* increased the number of flies exhibiting contractile irregularities (Figures S3H and S3I), a finding similar to what is seen in response to cardiac-specific knockdown of the *KCNQ* $K^+$ channel (Figure S3I) and what has been reported for *KCNQ* mutant flies (Ocorr et al., 2007b). Of note, a *not3 P* element mutant was developmentally lethal, exhibiting a late stage defect in embryonic heart tube organization, which could be rescued by *P* element excision (Figure S3C).

The CCR4-Not complex component *UBC4* was also a major hit identified by our heart screen. Moreover, *UBC4* expression was reduced after *not3* knockdown (Figure S3B). *Hand-Gal4>UAS-UBC4*-RNAi flies also exhibited significantly longer heart periods and showed dramatically altered diastolic and systolic diameters and reduced fractional shortening relative to control hearts (Figures 3C–3G). Fluorescent imaging again revealed severe myofibrillar disarray (Figure 4D) that was strikingly similar to that observed in *not3* knockdown hearts. Further, we observed similar structural and functional phenotypes in *not1* cardiac-specific knockdown flies (A.C., G.N., J.P., and R.B., unpublished data). Thus, knockdown of different components of the CCR4-Not complex result in abnormal heart structure and severely impaired cardiac function indicative of dilated cardiomyopathy.

### Functional Assessment of Additional *Drosophila* Heart Hits

To extend our confirmations beyond the CCR4-Not complex, we assayed heart function in adult flies with heart-specific knockdown of four additional candidates identified in our heart screen (Figure S3). One candidate heart gene tested was *CG1216* (*Mrityu*), which encodes a mesoderm-expressed BTB-POZ domain-containing protein (Rusconi and Challa, 2007). Cardiac knockdown of *CG1216* resulted in a significant increase in systolic diameter. Another candidate heart gene, *CG8933* (*extradenticle*), encodes a PBX-family transcription factor. Cardiac knockdown of *CG8933* resulted in increased systolic diameter and reduced fractional shortening. Cardiac knockdown of *CG33261* (*Trithorax-like*) resulted in significantly altered diastolic and systolic diameters as well as impaired fractional shortening. Finally, knockdown of *CG7371*, which encodes a Vps52 domain-containing protein predicted to participate in Golgi trafficking, resulted in a marked increase in heart period and affected the diastolic diameter. These data further demonstrate that our screen indeed has the capacity to identify novel factors involved in and required for normal adult heart function.

### Generation of *not3* Knockout Mice

We next tested whether our data on *Drosophila* can be directly translated into a mammalian species. The mouse and human NOT3 proteins (official gene name *Cnot3*) share 60% identity with the *Drosophila not3* ortholog. Expression of human and mouse *not3* messenger RNA (mRNA) transcripts can be found in the majority of tissues analyzed. Although *not3* is evolutionarily conserved from yeast to mammals, essentially nothing is known about the in vivo role of mammalian *not3*. We therefore generated *not3* knockout mice.

We disrupted the *not3* gene in murine embryonic stem cells (ESCs) using a targeting vector in which nucleotides encompassing exons 2 through 9 are deleted (Figure 5A and Figure S4A). Both $not3^{+/-}$ male and $not3^{+/-}$ female mice are viable and exhibit normal fertility. We never obtained viable $not3^{-/-}$ newborn mice, indicating that loss of *not3* results in embryonic lethality. We staged embryonic development but failed to recover *not3* null embryos from placental implantations (Figures S4B and S4C). We therefore assayed early embryogenesis and observed that $not3^{-/-}$ blastocysts can develop. These mutant blastocysts have a normal appearance (Figure S4D), occur at Mendelian frequencies (Figures S4E and S4F), and express key markers of early embryonic differentiation at normal levels (Figure S4G). *not3* mRNA transcripts and NOT3 protein were undetectable in $not3^{-/-}$ blastocysts by RT-PCR and immunostaining (Figures S4F and S4G). In $not3^{+/+}$ and $not3^{-/-}$ epiblast cultures (Figure S4H), trophoblast cells started to spread and supported the outgrowths of the inner cell mass (ICM). While the ICM of $not3^{+/+}$ blastocysts continued to grow, $not3^{-/-}$ ICM cells exhibited a severe outgrowth defect. Thus, complete loss of mouse *not3* results in early embryonic death at the implantation stage.

### *not3* Haploinsufficiency Results in Impaired Heart Function

We speculated that similar to RNAi-mediated downregulation of *not3* in *Drosophila*, *not3* haploinsufficiency might also reveal a role in mammalian heart function. In *not3* heterozygote mice, *not3* expression is indeed downregulated in the heart (Figure 5B). We failed to observe overt structural changes in the hearts of $not3^{+/-}$ mice. However, both male and female *not3* haploinsufficient mice exhibited a reduction in cardiac contractility as determined by decreased left ventricle fractional shortening and increased left ventricular diameter in systole (Figures 5C and 5D).

To address whether the defects in cardiac function are intrinsic to the heart per se or whether the observed impairment of contractility was secondary because of haploinsufficiency of *not3* in other tissues, we subjected explanted hearts from wild-type and $not3^{+/-}$ littermate mice to Langendorff perfusion, assessing ex vivo heart function (Joza et al., 2005). When isoproterenol was used to activate β-adrenergic receptors, $not3^{+/-}$ hearts exhibited severe contractile abnormalities as defined by impaired generation of left ventricular pressure (LVP) (Figure 5E and Figure S5A). Hemodynamic measurements confirmed that all functional heart parameters such as $dP/dT_{max}$ or $dP/dT_{min}$, indicative of generated contractile pressure, were markedly reduced in $not3^{+/-}$ hearts (data not shown). Moreover, when explanted hearts were electrically stimulated, $not3^{+/-}$ hearts exhibited a striking defect in contractility (Figure 5F). Thus, downregulation of *not3* expression in *not3* haploinsufficient mice results in an intrinsic impairment in heart function.

Yeast strains mutant for components of the CCR4-Not complex, including *not3*, display reduced acetylation levels of lysine residues on histone tails (e.g., H3K9) (Peng et al., 2008) and/or reduced trimethylation of H3K4 (Laribee et al., 2007). H3K9 acetylation and H3K4 trimethylation are indicative of transcriptionally active states of chromatin. Moreover, promoter regions of NOT3 target genes were shown to recruit trimethylated H3K4 in mouse ESCs (Hu et al., 2009), suggesting that NOT3 may regulate chromatin modifications. Our gene expression and bioinformatic analyses of mouse *not3* knockout cells revealed that histone deacetylases (HDACs) and mRNA metabolisms are localized central in gene networks (K.K., unpublished data). We therefore assessed the state of histone modifications in hearts from $not3^{+/-}$ mice. Histone extracts of whole hearts from *not3* haploinsufficient mice showed a slight but significant reduction in active histone marks such as acetylation of H3K9 and trimethylation of H3K4 (Figures 5G and 5H and Figure S5). H3K27 trimethylation was not changed (Figure 5I and Figure S5). Treatment of $not3^{+/-}$ hearts with the HDAC inhibitor VPA restored the reduced acetylation of H3K9 and H3K4 trimethylation to that of wild-type levels (Figures 5G–5I and Figure S5). Most importantly, administration of HDAC inhibitors rescued the impairment in heart function in $not3^{+/-}$ mice; i.e., ex vivo heart functions of VPA treated mice were similar to control mice in response to both isoproterenol (Figure 5J) and electrical stimulation (Figure 5K). These data were confirmed with TSA, a second HDAC inhibitor (Figures S5H and S5I). Together, these data show that $not3^{+/-}$ mice exhibit a spontaneous and intrinsic defect in cardiac function that can be rescued with HDAC inhibitors.

### $not3^{+/}$ Mice Develop Severe Cardiomyopathy in Response to Cardiac Stress

We next exposed control and $not3^{+/-}$ littermates to chronic pressure overload by surgical constriction of the aorta (transverse aortic constriction, TAC). Three weeks after TAC, heart weight/body weight ratios (HW/BW) increased in both $not3^{+/+}$ and $not3^{+/-}$ mice, although this increase was significantly larger in the $not3^{+/}$ mice (Figure 6A). Cardiac hypertrophy was also seen by histology (Figure 6D and Figure S6A). Aortic banding of $not3^{+/-}$ mice resulted in severe heart failure characterized by decreased fractional shortening (Figure 6B) and a dilation of the left ventrical as determined by echocardiography (Figure 6C). In addition, $not3^{+/-}$ mice develop severe cardiac fibrosis after TAC, as shown by Masson-trichrome staining of hearts 3 weeks after TAC (Figure 6D and Figure S6B). Thus, $not3^{+/-}$ mice develop severe symptoms of heart failure in response to cardiac stress.

We next assessed whether HDAC inhibitors can also rescue stress-induced heart failure. HDAC inhibitor treatment could indeed block the augmented loss of cardiac function observed in $not3^{+/-}$ mice after TAC (Figures 7A and 7B). In vivo treatment of $not3^{+/-}$ mice with HDAC inhibitors also blocked the exaggerated induction of heart failure markers such as *ANF* (Figure S6C) and *βMyhc* (Figure S6D). Moreover, treatment with an HDAC inhibitor restored the observed histone alterations in $not3^{+/-}$ mice to that of wild-type littermates (Figure 7C and Figures S6E and S6F). Thus, *not3* haploinsufficiency results in exaggerated heart failure that can be rescued by HDAC inhibition in vivo.

### A Common Genomic Variant in the *NOT3* Promoter Correlates with Cardiac Repolarization Duration in Humans

Using an in silico search to identify NOT3 target genes, we found that NOT3 has been shown to bind to the *Kcnq1* promoter in

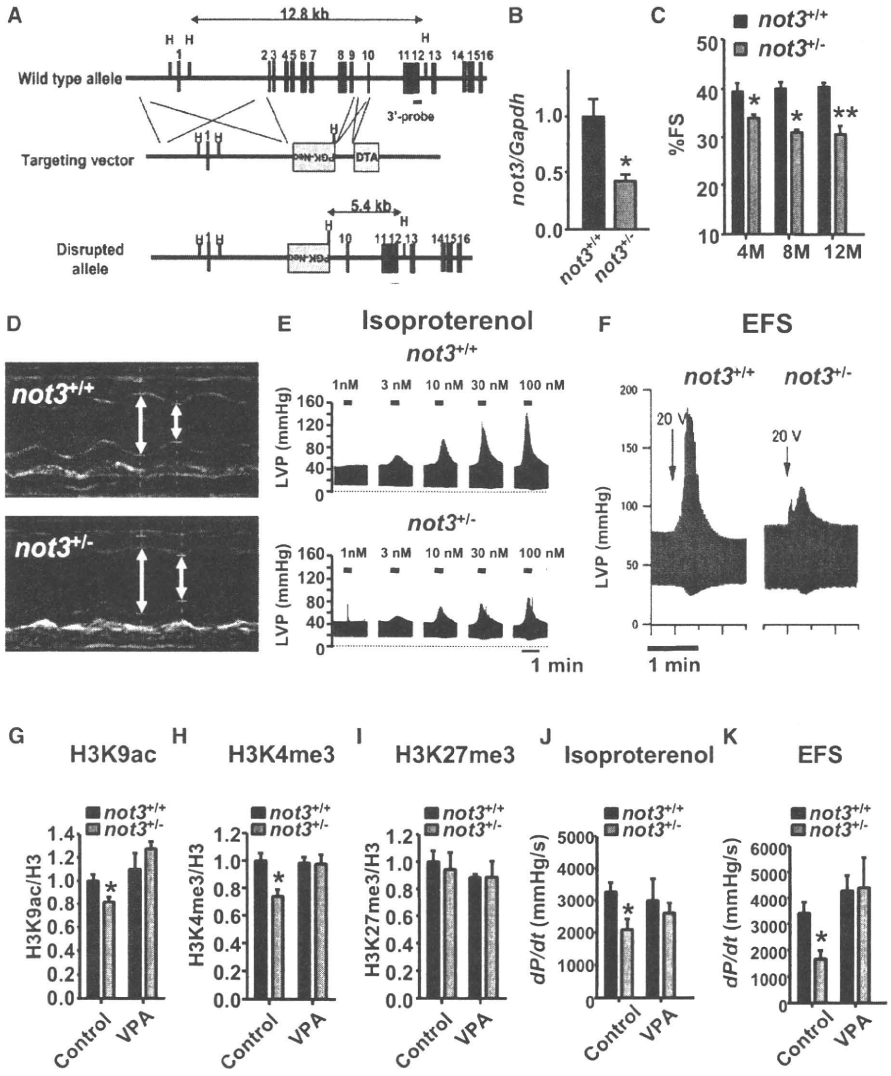


**Figure 5. *not3*$^{+/}$ Mice Exhibit Reduced Heart Contractility, Ex Vivo Function, and Histone Modifications that Can Be Rescued by Treatment with HDAC Inhibitors**

(A) Gene targeting strategy. Exons 2 to 9 of the *not3* gene (official symbol *cnot3*) were replaced with a PGK-Neo cassette by homologous recombination in A9 ESCs. The wild-type allele, targeting vector, mutant allele, and PGK-Neo and DTH selection cassettes are shown. Blue boxes indicate exons.

(B) Real-time PCR analyses for *not3* mRNA expression in 3-month-old wild-type and *not3*$^{+/-}$ hearts. Values were normalized to *gapdh* mRNA expression. n = 6 mice per group.

(C) *not3*$^{+/-}$ mice display a significant reduction in percent fractional shortening at 4 months of age, which became more pronounced with age. n = 6–8 mice per group. Fractional shortening was determined by echocardiography.

(D) Representative M mode echocardiography for wild-type and *not3*$^{+/-}$ mice at 8 months of age.

(E) Left ventricular pressure (LVP) measurements in isolated ex vivo *not3*$^{+/-}$ and *not3*$^{+/+}$ hearts under isoproterenol perfusion. *not3*$^{+/-}$ hearts from 4-month-old mice showed impaired contractile responses to different doses of isoproterenol perfusion in the retrograde Langendorff mode as compared to age-matched controls.

(F) Impaired contractile response of ex vivo *not3*$^{+/-}$ hearts to electrical field stimulation (EFS) compared with littermate *not3*$^{+/+}$ hearts. Representative data for left ventricular pressure (LVP) at 20 V stimulation are shown.

(G–I) H3K9 acetylation (H3K9ac) (G), H3K4 trimethylation (H3K4me3) (H), and H3K27 trimethylation (H3K27me3) (I) levels were analyzed by western blot for acid-extracted histones from whole heart ventricles of wild-type and *not3*$^{+/-}$ mice treated with vehicle or VPA (0.71% w/v in drinking water for 1 week) Band intensities were normalized to total H3 levels.

(J and K) Treatment (1 week) with the HDAC inhibitor VPA rescue impaired ex vivo heart contractility of *not3*$^{+/-}$ hearts to isoproterenol (100 nM) perfusion or 25 V EFS.

All values are mean ± SEM. *p < 0.05; **p < 0.01. n = 5–12 per group. See also Figures S4 and S5.

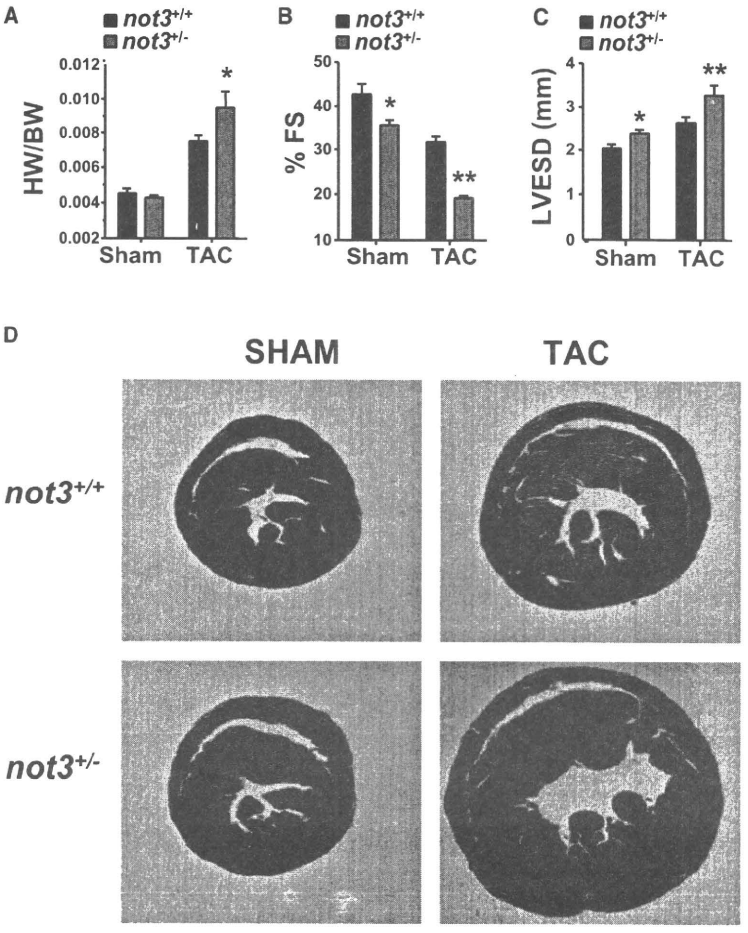


**Figure 6. *Not3*$^{+/}$ Mice Exhibit Severe Heart Failure in Response to Pressure Overload**

(A) Heart weight to body weight ratios (HW/BW) in *not3*$^{+/-}$ and *not3*$^{+/+}$ littermate mice 3 weeks after transverse aortic constriction (TAC). Animals receiving sham surgery are shown as controls.

(B and C) Echocardiography of male *not3*$^{+/-}$ and wild-type littermates 3 weeks after TAC. *not3*$^{+/-}$ mice with TAC show decreased percent fractional shortening (%FS) (B) and increased left ventricular diameter in systolic phase (LVESD) (C) compared with *not3*$^{+/+}$ mice that received TAC. All values are mean ± SEM. *$p < 0.05$; **$p < 0.01$.

(D) Representative sections of *not3*$^{+/+}$ and *not3*$^{+/-}$ hearts analyzed 3 weeks after sham or TAC surgery. Masson-trichrome stainings are shown to visualize collagen deposits indicative of fibrotic changes. Note the severe cardiac hypertrophy and ventricular dilation in *not3*$^{+/-}$ mice after TAC.

ESCs (Hu et al., 2009). *Kcnq1* encodes the α subunit of the repolarizing voltage gated potassium channel $I_{Ks}$, mutations in which are the most common cause of long-QT syndrome (LQT1) in humans (Wang et al., 1996). Abnormalities of cardiac repolarization, measured as alterations in QT interval, predispose to sudden cardiac death in humans (Moss and Kass, 2005). Indeed, while sham-operated *not3*$^{+/-}$ mice exhibit a subtle reduction in cardiac *Kcnq1* expression, this decrease was pronounced after TAC (Figure 7D). Reduced *Kcnq1* expression was rescued after HDAC inhibitor treatment. Also, for *Kcne1*, the β subunit of $I_{Ks}$, we observed a TAC-inducible and HDAC-sensitive defect in expression in *not3*$^{+/-}$ hearts (Figure 7E). In fly *not3*-RNAi hearts, *KCNQ* expression is also reduced (Figure S3D), and these flies exhibit cardiac contractile irregularities (Figures S3H and S3I).

Recently, two consortia have published genome-wide association studies (GWAS) for QT interval, QT-Interval and Sudden Cardiac Death (QTSCD) (Pfeufer et al., 2009) and Genetics of QT-Interval (QTGEN) (Newton-Cheh et al., 2009). One of the 12 identified genomic regions contains the *NOT1* gene, which we also found as a hit in our *Drosophila* screen (Figures 3A and 3B). Because of the stringent requirements to achieve a genome-wide significance threshold of $p < 5 \times 10^{-8}$ (Dudbridge and Gusnanto, 2008), many genuinely associated alleles will be missed because of both a failure to exceed this statistical threshold and the absence of functional confirmatory data for genes within loci of interest. We therefore evaluated whether common variants in and near the human *NOT3* locus are also associated with alterations in QT interval. Intriguingly, SNP rs36643 (chromosome 19: 59.3 Mb), located in the promoter region ~969 base pairs upstream from the *NOT3* transcriptional start site (924 bases upstream of the TATA box), is significantly associated with QT interval in the QTSCD data set (Figure 7F). Patients carrying the common T allele (minor allele frequency = 0.65) showed a dose-dependent increase in QT interval (ES = +1.03 ± 0.29 ms QT interval per copy of T allele, $p = 3.66E^{-04}$) (Figure 7G). Of note, similar to adult *kcnq1* mutant mice (Nerbonne, 2004), we did not observe an increased QT interval in *not3* heterozygous mice (except for one mouse with arrhythmia, K.K., M.M., H.Y., and K.F., unpublished data). Thus, our genome-wide screening data for death in flies can be used to identify candidate variants in humans that predispose individuals to heart disease, i.e., in the case of *NOT3* to arrhythmia and sudden death.

## DISCUSSION

Here, we present the first in vivo RNAi adult heart screen in *Drosophila* assaying conserved genes. Using functional imaging, we were able to observe cardiac defects in all flies with heart-specific knockdown of candidate genes evaluated to date. Our experimental approach to screen for conserved heart genes in *Drosophila* in concert with advanced bioinformatics has the potency to reveal human and mouse genes involved in heart function and heart disease. Moreover, we uncovered a plethora of additional genes, a large proportion of which had

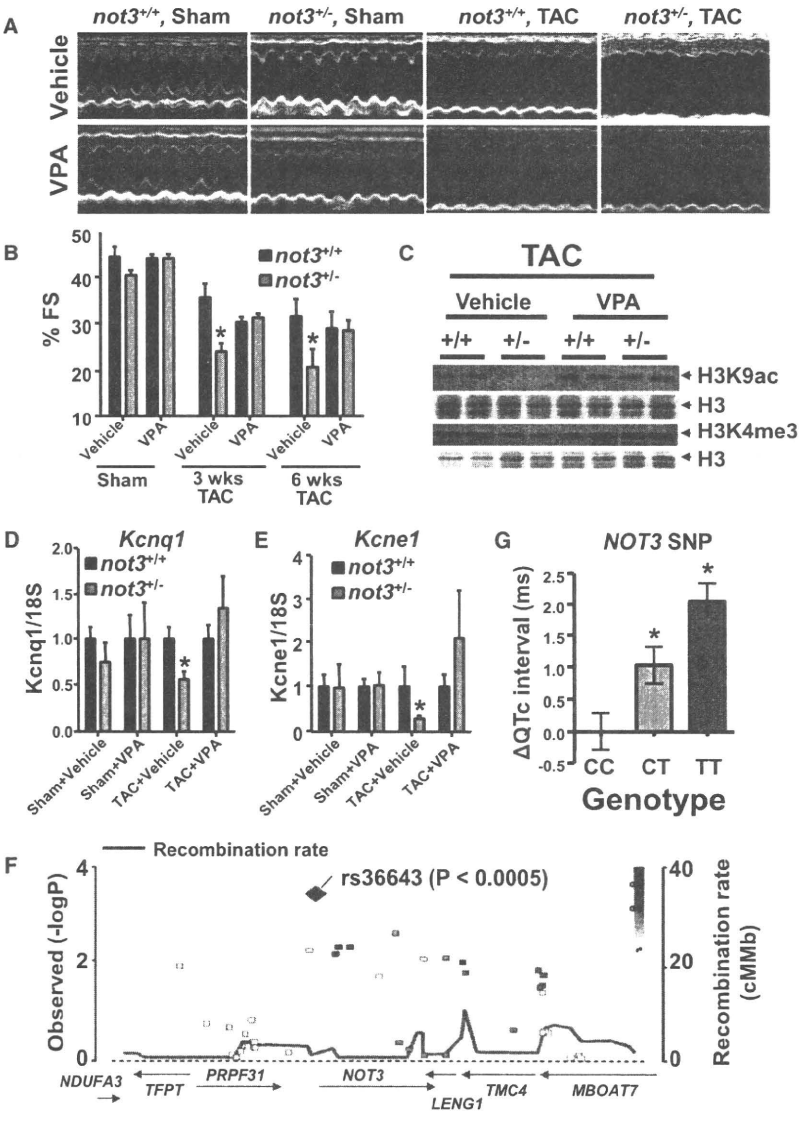


**Figure 7. *not3* Is a Conserved Regulator of Heart Function**

(A and B) Rescue of severe heart failure in TAC $not3^{+/-}$ hearts by the HDAC inhibitor VPA. One day after TAC or sham surgery, the mice received treatment with vehicle or VPA (0.71% w/v in drinking water) for 6 weeks. Representative M mode echocardiography (A) and percent FS (B) in $not3^{+/-}$ and $not3^{+/+}$ littermate mice 6 weeks after TAC or sham surgery with or without VPA treatment are shown. Values are mean ± SEM. *$p < 0.05$.

(C) Reduced H3K9 acetylation (H3K9ac) and H3K4 trimethylation (H3K4me3) levels were rescued by VPA treatment. Acid-extracted histones from the hearts 6 weeks after TAC surgery were immunoblotted with antibodies for H3K9ac and H3K4me3. H3 is shown as a loading control.

(D and E) Real-time PCR analyses for the QT interval-associated potassium channel genes *Kcnq1* and *Kcne1*. Total RNA was isolated from hearts 6 weeks after TAC or sham surgery with or without VPA treatment, and *Kcnq1* and *Kcne1* mRNA levels were measured and normalized to *18S* mRNA. Data are shown as fold changes compared to $not3^{+/+}$ mice for each treatment group. Values are mean ± SEM. *$p < 0.05$; **$p < 0.01$. $n = 5–10$ per group.

(F) Regional visualization of the association signal between common variants in the *NOT3* region and the adjusted QT interval (QTc). SNP rs36643 in the 5′ region of *NOT3* (−969 bp from the transcription start and −924 bp from the TATA box) showed a significant regional association ($p = 0.000366$).

(G) Association between the T allele of SNP rs36643 and a prolongation of QTc. * $p < 0.0005$ from linear regression with inverse variance weighting using an additive genetic model. Data are derived from a meta-analysis of genome-wide association scans in several populations (Pfeufer et al., 2009).

See also Figure S6.

completely unknown functions until now. Future experiments are required to test whether our candidate genes indeed control cardiac development, regulate adult heart function, and/or influence the outcome of heart failure in response to cardiac stress.

One pathway we identified was the CCR4-Not complex. Functional heart analyses in *Drosophila* confirmed that RNAi-mediated silencing of the CCR4-Not components *not3* and *UBC4* resulted in a severe impairment of cardiac function that resembles dilated cardiomyopathy in experimental mouse models and human patients. To provide a first proof of principle that our fly hits can indeed have similar functions in the more complex mammalian heart, we generated knockout mice for a component of the CCR4-Not complex. *not3* haploinsufficient mice develop spontaneous impairment of heart function and severe heart failure after aortic banding. Mechanistically, *not3* downregulation results in a defect in active histone marks and cardiac defects observed in $not3^{+/-}$ mice could be rescued by treatment with HDAC inhibitors. Besides regulating transcriptionally active states of chromatin (Hu et al., 2009; Jayne et al., 2006; Laribee et al., 2007; Peng et al., 2008), the CCR4-Not complex has also been implicated in RNA deadenylation (Tucker et al., 2001) and microRNA-mediated mRNA degradation (Behm-Ansmant et al., 2006). Thus, we cannot exclude that CCR4-Not components affect additional mechanisms regulating heart function. Importantly, our work on *not3* in flies and mice has also allowed us to identify a single-nucleotide polymorphism in the human *NOT3* promoter that is associated with prolonged QT intervals and sudden cardiac death in humans. Thus, large-scale screens in *Drosophila* can be directly translated to

mammalian species and, in combination with other genome-wide approaches, can reveal regulators of heart function and heart failure.

## EXPERIMENTAL PROCEDURES

Detailed experimental procedures are provided in the Extended Experimental Procedures.

### Fly Stocks

All RNAi transgenic fly lines were obtained from the Vienna *Drosophila* RNAi Center (VDRC) RNAi stocks (Dietzl et al., 2007). The cardiac tissue-specific *TinCΔ4 12a-Gal4* was a kind gift from Manfred Frasch, (Lo and Frasch, 2001) and *Hand-Gal4* was a gift from Eric Olsen (Han and Olson, 2005).

### Screening System

Transgenic RNAi males were crossed to *TinCΔ4* virgin females. Viable lines were then incubated at 29°C for 6 days to expose flies to temperature stress (Paternostro et al., 2001). Initially, a Z score cutoff of 2 (mean control-test)/SD was used to select RNAi lines for retesting.

### *Drosophila* Cardiac Function, Morphology, and Gene Expression

*UAS*-RNAi fly lines obtained from the Vienna *Drosophila* RNAi Center were crossed to *Hand-Gal4* (II) driver flies and to $w^{1118}$ wild-type control flies. Flies were assessed for heart morphology and physiology with high-speed digital video imaging (Ocorr et al., 2007b). M modes were generated and cardiac parameters including heart periods, diastolic and systolic diameters, and fractional shortening were recorded for each group with a MatLab-based image analysis program (Fink et al., 2009). Fluorescent imaging of *Drosophila* heart tubes was performed as described (Alayari et al., 2009).

### Bioinformatics Analysis

For a detailed description of full bioinformatics analysis, please see the Extended Experimental Procedures.

### Phenotyping of *not3* Knockout Mice

A targeting vector was constructed to replace exons 2 and 9 of the murine *not3* gene. Fractional shortening (FS) was calculated as follows: FS = [(LVEDD − LVESD)/LVEDD] × 100. For ex vivo heart studies, hearts were assayed with a Langendorff apparatus. The heart was paced electrically at 400 beats/min (bpm), and the electrical field stimulation (EFS) was applied in conjunction with the pacing stimulation. Isoproterenol was perfused for 30 s with the indicated doses. For HDAC inhibition, wild-type and $not3^{+/-}$ mice were treated with vehicle, Trichostatin A (TSA), or Valproic acid (VPA) for 1 week. Acid-extracted histones were prepared, resolved, and transferred to nitrocellulose membranes for western blotting. Transverse aorta constriction (TAC) was performed as described (Kuba et al., 2007). For heart histology, hearts were arrested, fixed, embedded in paraffin, and stained with hematoxylin and eosin (H&E) or Masson-Trichrome.

### Human QT Interval Association

Human QT interval association signals over the NOT3 region were obtained from data generated by the QTSCD Consortium (Pfeufer et al., 2009).

## SUPPLEMENTAL INFORMATION

Supplemental Information includes Extended Experimental Procedures, six figures, five tables, and one movie and can be found with this article online at doi:10.1016/j.cell.2010.02.023.

## ACKNOWLEDGMENTS

We thank all members of our laboratories and the VDRC, the Bioscience Education Research Center (Akita University), and Vincent Chen for helpful discussions and excellent technical support. We thank Eric Olson for the *Hand-Gal4* driver and Manfred Frasch for *TinCΔ4-Gal4* driver stocks. We thank the members of the QTSCD consortium for valuable support and discussion. J.M.P. is supported by the IMBA, the Austrian Ministry of Science, a European Research Council Advanced Investigator grant, and EuGeneHeart. K.K. is supported by Kaken (21659198) from the Japanese Ministry of Science, the Medical Top Track Program, and the Japan Heart Foundation. G.G.N. was supported by a Marie Curie International Incoming Fellowship. A.C. was supported by a postdoctoral fellowship and K.O. by a Scientist Development Grant from the American Heart Association. R.B. was supported by grants from the National Heart, Lung, and Blood Institute of the National Institutes of Health. A.P. is supported by grants 01GR0803 and 01EZ0874 from the German Federal Ministry of Research, FSID-261/2008 from the UK Foundation for the Study of Infant Deaths, and YGEIA/1104/17 and ERYEX/0406/06 from the Cyprus Cardiovascular Disease Educational and Research Trust. Y.I. is supported by the Global Center of Excellence Program.

Received: May 4, 2009
Revised: October 20, 2009
Accepted: February 2, 2010
Published: April 1, 2010

## REFERENCES

A.H.A. (2005). http://www.americanheart.org/.

Alayari, N.N., Vogler, G., Taghli-Lamallem, O., Ocorr, K., Bodmer, R., and Cammarato, A. (2009). Fluorescent Labeling of *Drosophila* Heart Structures. J. Vis. Exp. 10.3791/1423.

Albert, T.K., Lemaire, M., van Berkum, N.L., Gentz, R., Collart, M.A., and Timmers, H.T. (2000). Isolation and characterization of human orthologs of yeast CCR4-NOT complex subunits. Nucleic Acids Res. *28*, 809–817.

Behm-Ansmant, I., Rehwinkel, J., Doerks, T., Stark, A., Bork, P., and Izaurralde, E. (2006). mRNA degradation by miRNAs and GW182 requires both CCR4:NOT deadenylase and DCP1:DCP2 decapping complexes. Genes Dev. *20*, 1885–1898.

Bodmer, R. (1995). Heart development in Drosophila and its relationship to vertebrates. Trends Cardiovasc. Med. *5*, 21–28.

Cripps, R.M., and Olson, E.N. (2002). Control of cardiac development by an evolutionarily conserved transcriptional network. Dev. Biol. *246*, 14–28.

Denis, C.L. (1984). Identification of new genes involved in the regulation of yeast alcohol dehydrogenase II. Genetics *108*, 833–844.

Dietzl, G., Chen, D., Schnorrer, F., Su, K.C., Barinova, Y., Fellner, M., Gasser, B., Kinsey, K., Oppel, S., Scheiblauer, S., et al. (2007). A genome-wide transgenic RNAi library for conditional gene inactivation in Drosophila. Nature *448*, 151–156.

Dudbridge, F., and Gusnanto, A. (2008). Estimation of significance thresholds for genomewide association scans. Genet. Epidemiol. *32*, 227–234.

Fink, M., Callol-Massot, C., Chu, A., Ruiz-Lozano, P., Izpisua Belmonte, J.C., Giles, W., Bodmer, R., and Ocorr, K. (2009). A new method for detection and quantification of heartbeat parameters in Drosophila, zebrafish, and embryonic mouse hearts. Biotechniques *46*, 101–113.

Gordon, T., Castelli, W.P., Hjortland, M.C., Kannel, W.B., and Dawber, T.R. (1977). Predicting coronary heart disease in middle-aged and older persons. The Framington study. JAMA *238*, 497–499.

Han, Z., and Olson, E.N. (2005). Hand is a direct target of Tinman and GATA factors during Drosophila cardiogenesis and hematopoiesis. Development *132*, 3525–3536.

Hu, G., Kim, J., Xu, Q., Leng, Y., Orkin, S.H., and Elledge, S.J. (2009). A genome-wide RNAi screen identifies a new transcriptional module required for self-renewal. Genes Dev. *23*, 837–848.

Jayne, S., Zwartjes, C.G., van Schaik, F.M., and Timmers, H.T. (2006). Involvement of the SMRT/NCoR-HDAC3 complex in transcriptional repression by the CNOT2 subunit of the human Ccr4-Not complex. Biochem. J. *398*, 461–467.

Joza, N., Oudit, G.Y., Brown, D., Bénit, P., Kassiri, Z., Vahsen, N., Benoit, L., Patel, M.M., Nowikovsky, K., Vassault, A., et al. (2005). Muscle-specific

loss of apoptosis-inducing factor leads to mitochondrial dysfunction, skeletal muscle atrophy, and dilated cardiomyopathy. Mol. Cell. Biol. *25*, 10261–10272.

Kuba, K., Zhang, L., Imai, Y., Arab, S., Chen, M., Maekawa, Y., Leschnik, M., Leibbrandt, A., Markovic, M., Makovic, M., et al. (2007). Impaired heart contractility in Apelin gene-deficient mice associated with aging and pressure overload. Circ. Res. *101*, e32–e42.

Lakatta, E.G., and Levy, D. (2003). Arterial and cardiac aging: major shareholders in cardiovascular disease enterprises: Part II: the aging heart in health: links to heart disease. Circulation *107*, 346–354.

Laribee, R.N., Shibata, Y., Mersman, D.P., Collins, S.R., Kemmeren, P., Roguev, A., Weissman, J.S., Briggs, S.D., Krogan, N.J., and Strahl, B.D. (2007). CCR4/NOT complex associates with the proteasome and regulates histone methylation. Proc. Natl. Acad. Sci. USA *104*, 5836–5841.

Lloyd-Jones, D., Adams, R., Carnethon, M., De Simone, G., Ferguson, T.B., Flegal, K., Ford, E., Furie, K., Go, A., Greenlund, K., et al. American Heart Association Statistics Committee and Stroke Statistics Subcommittee. (2009). Heart disease and stroke statistics—2009 update: a report from the American Heart Association Statistics Committee and Stroke Statistics Subcommittee. Circulation *119*, e21–e181.

Lo, P.C., and Frasch, M. (2001). A role for the COUP-TF-related gene seven-up in the diversification of cardioblast identities in the dorsal vessel of Drosophila. Mech. Dev. *104*, 49–60.

Morita, H., Seidman, J., and Seidman, C.E. (2005). Genetic causes of human heart failure. J. Clin. Invest. *115*, 518–526.

Moss, A.J., and Kass, R.S. (2005). Long QT syndrome: from channels to cardiac arrhythmias. J. Clin. Invest. *115*, 2018–2024.

Mudd, J.O., and Kass, D.A. (2008). Tackling heart failure in the twenty-first century. Nature *451*, 919–928.

Nabel, E.G. (2003). Cardiovascular disease. N. Engl. J. Med. *349*, 60–72.

Nerbonne, J.M. (2004). Studying cardiac arrhythmias in the mouse—a reasonable model for probing mechanisms? Trends Cardiovasc. Med. *14*, 83–93.

Newton-Cheh, C., Eijgelsheim, M., Rice, K.M., de Bakker, P.I., Yin, X., Estrada, K., Bis, J.C., Marciante, K., Rivadeneira, F., Noseworthy, P.A., et al. (2009). Common variants at ten loci influence QT interval duration in the QTGEN Study. Nature genetics *41*, 399–406.

Ocorr, K., Perrin, L., Lim, H.Y., Qian, L., Wu, X., and Bodmer, R. (2007a). Genetic control of heart function and aging in Drosophila. Trends Cardiovasc. Med. *17*, 177–182.

Ocorr, K., Reeves, N.L., Wessells, R.J., Fink, M., Chen, H.S., Akasaka, T., Yasuda, S., Metzger, J.M., Giles, W., Posakony, J.W., and Bodmer, R. (2007b). KCNQ potassium channel mutations cause cardiac arrhythmias in Drosophila that mimic the effects of aging. Proc. Natl. Acad. Sci. USA *104*, 3943–3948.

Paternostro, G., Vignola, C., Bartsch, D.U., Omens, J.H., McCulloch, A.D., and Reed, J.C. (2001). Age-associated cardiac dysfunction in Drosophila melanogaster. Circ. Res. *88*, 1053–1058.

Peng, W., Togawa, C., Zhang, K., and Kurdistani, S.K. (2008). Regulators of cellular levels of histone acetylation in Saccharomyces cerevisiae. Genetics *179*, 277–289.

Pfeufer, A., Sanna, S., Arking, D.E., Müller, M., Gateva, V., Fuchsberger, C., Ehret, G.B., Orrú, M., Pattaro, C., Köttgen, A., et al. (2009). Common variants at ten loci modulate the QT interval duration in the QTSCD Study. Nat. Genet. *41*, 407–414.

Qian, L., and Bodmer, R. (2009). Partial loss of GATA factor Pannier impairs adult heart function in Drosophila. Hum. Mol. Genet. *18*, 3153–3163.

Qian, L., Mohapatra, B., Akasaka, T., Liu, J., Ocorr, K., Towbin, J.A., and Bodmer, R. (2008). Transcription factor neuromancer/TBX20 is required for cardiac function in Drosophila with implications for human heart disease. Proc. Natl. Acad. Sci. USA *105*, 19833–19838.

Ray, V.M., and Dowse, H.B. (2005). Mutations in and deletions of the Ca2+ channel-encoding gene cacophony, which affect courtship song in Drosophila, have novel effects on heartbeating. J. Neurogenet. *19*, 39–56.

Rusconi, J.C., and Challa, U. (2007). Drosophila Mrityu encodes a BTB/POZ domain-containing protein and is expressed dynamically during development. Int. J. Dev. Biol. *51*, 259–263.

Sanguinetti, M.C., and Tristani-Firouzi, M. (2006). hERG potassium channels and cardiac arrhythmia. Nature *440*, 463–469.

Sanyal, S., Jennings, T., Dowse, H., and Ramaswami, M. (2006). Conditional mutations in SERCA, the Sarco-endoplasmic reticulum Ca2+-ATPase, alter heart rate and rhythmicity in Drosophila. J. Comp. Physiol. [B] *176*, 253–263.

Tucker, M., Valencia-Sanchez, M.A., Staples, R.R., Chen, J., Denis, C.L., and Parker, R. (2001). The transcription factor associated Ccr4 and Caf1 proteins are components of the major cytoplasmic mRNA deadenylase in Saccharomyces cerevisiae. Cell *104*, 377–386.

Wang, Q., Curran, M.E., Splawski, I., Burn, T.C., Millholland, J.M., VanRaay, T.J., Shen, J., Timothy, K.W., Vincent, G.M., de Jager, T., et al. (1996). Positional cloning of a novel potassium channel gene: KVLQT1 mutations cause cardiac arrhythmias. Nat. Genet. *12*, 17–23.

Yusuf, S., Reddy, S., Ounpuu, S., and Anand, S. (2001). Global burden of cardiovascular diseases: part I: general considerations, the epidemiologic transition, risk factors, and impact of urbanization. Circulation *104*, 2746–2753.

# Supplemental Information

## EXTENDED EXPERIMENTAL PROCEDURES

### Fly Stocks

All RNAi transgenic fly lines were obtained from the VDRC RNAi stocks. The whole genome VDCR library has been previously reported (Dietzl et al., 2007). The cardiac-tissue specific *TinCΔ4 12a-Gal4* was kind gift from Manfred Frasch, (Lo and Frasch, 2001) and *Hand-Gal4* was kind gift from Eric Olsen, (Han and Olson, 2005) driver lines have been previously described and used to study genes involved in *Drosophila* heart development and cardiac function in adult flies (Wolf et al., 2006). $w^{1118}$ wild-type control flies obtained from the VDRC were used when indicated since the *Drosophila melanogaster* $w^{1118}$ background is isogenic to the VDRC RNAi library. The fly stock for the *not3* associated P-element ($CG8426^{KG10496}$) was obtained from Bloomington (#15271).

### Screening System

Transgenic *UAS*-RNAi males were crossed to *TinCΔ4 12a-Gal4* virgin females and 4 day old viable F1 adult progeny were transferred to test chambers containing 2 filter pads with 2 ml of a 50 mMol sucrose solution. The viable RNAi lines were then incubated at 29°C for 6 days to expose flies to temperature stress as described previously (Paternostro et al., 2001) and the number of dead and surviving flies were counted. Initially a Z-score cut-off of 2 (Mean control-test)/SD was used to select RNAi lines for re-testing. Developmental lethality was assessed in a semiquantitative fashion, with lethal crosses scored as 0, semi-lethal crosses scored as 0.5, and viable crosses scored as 1. During re-testing, lethality was staged when apparent. In all cases, crosses were scored based on the furthest developmental stage reached: 0 = lethal (embryonic lethal or no off-spring), 1 = larval lethal, 2 = pupal lethal, 3 = adult lethal (die within 4 days after eclosion), 4 = adult viable.

### *Drosophila* Cardiac Analysis

*UAS*-RNAi fly lines obtained from the VDRC were crossed to *Hand-Gal4* (II) driver-flies and to $w^{1118}$ wild-type control flies. As an additional control, *Hand-Gal4* (II) driver-flies were crossed to $w^{1118}$ wild-type flies. The progeny were raised at 25°C on standard cornmeal-agar medium. At 1 week of age, 29-40 female offspring from each cross were anaesthetized and dissected. All procedures were done at room temperature (18-22°C) as previously described (Cammarato et al., 2008; Ocorr et al., 2007). Briefly, each head, ventral thorax and ventral abdominal cuticle was removed exposing the abdomen. All internal organs and abdominal fat were removed leaving only the heart and associated muscles for each fly. Dissections were performed in oxygenated artificial adult hemolymph. The semi-intact preparations were allowed to equilibrate with oxygenation for 20–30 min prior to filming. Analysis of gross heart morphology and physiology was performed using high speed movies. 30 s movies were taken at rates of 100–200 frames/sec using a Hamamatsu EM-CCD digital camera on a Leica DM LFSA microscope with a 10x immersion lens. All images were acquired and contrast enhanced using Simple PCI imaging software (Compix, Inc.). M-modes were generated and determination of cardiac parameters, including heart periods, diastolic and systolic diameters and fractional shortening for each group was performed using a MatLab-based image analysis program (Fink, 2009). ANOVA of genotype as a function of each measured cardiac parameter was employed to test for significant differences between $w^{1118}$>*UAS-Not3*-RNAi or $w^{1118}$>*UAS-UBC4*-RNAi control flies and both *Hand-Gal4*>*UAS-Not3*-RNAi or the *Hand-Gal4*>*UAS-UBC4*-RNAi mutants, respectively. Additionally, one-way ANOVAs with Bonferroni multiple comparison post tests were employed to determine if significant differences between $w^{1118}$>*Hand-Gal4* and all $w^{1118}$>*UAS*-RNAi control lines were present.

### Fluorescent Staining

Fluorescent staining and imaging of *Drosophila* heart tubes were performed as described (Alayari et al., 2009). Briefly, beating hearts of semi-intact *Drosophila* were placed in artificial adult *Drosophila* hemolymph containing 10mM EGTA. Cardiac tubes were examined to ensure contractions were inhibited. Hearts were fixed in 1xPBS containing 4% formaldehyde at room temperature for 20 min with gentle shaking. Washing of hearts was performed three times for 10 min with PBSTx (PBS containing 0.1% Triton X-100) at room temperature with continual shaking. After washing, the hearts were incubated with Alexa584-phalloidin in PBSTx (1:1000) for 20 min with continual agitation. Washing of the hearts was carried out three times for 10 min with PBSTx at room temperature. The hearts were rinsed in 100 µl of PBS for 10 min. The specimens were mounted on microscope slides and viewed at 10X magnification using a Zeiss Imager Z1 fluorescent microscope equipped with an Apotome sliding module.

### Q-RT-PCR of *Drosophila* Cardiac Associated Transcripts

Quantitative RT-PCR was performed using standard procedures according to (Akasaka et al., 2006) with minor modifications. Total RNA was extracted from 30 hearts per genotype (all female flies). Quantitative Real Time-PCR was performed with the LightCycler FastStart DNA Master PLUS SYBR Green I kit (Roche) using single strand cDNA."

The primer sets were as follows:

*not3*_05 CGCAAAGCAGTATCGGAAGT
*not3*_06 CCGCAGGATTGTTACCAG
*UBC4*_01 CGCAGCTTTGTGTTTCGTTT
*UBC4*_02 GTTGGTGTCTCGCGTATT

*SERCA*_01 CAAGTCCTACTCGGGTCGTG
*SERCA*_02 CATAGCGGAGATTTCGTTCAT
*KCNQ*_11 ACCATCAAGGAGTACGAAGA
*KCNQ*_12 CGATGACCAGAGTCGAG
*Mhc*_01 AGTCCGAGCGTCGCGTCAAG
*Mhc*_02 TGAGGGCGGCGATTTC
*rp49*_01 GAC GCT TCA AGG GAC AGT ATC TG
*rp49*_02 AAA CGC GGT TCT GCA TGA G
*actin*_01 ATCCGCAAGGATCTGTATGC
*actin*_02 ACATCTGCTGGAAGGTGGAC
*actinin*_03 CCTGACCGCCAACGACATGA
*actinin*_04 CATTTGCCGCTCGATCCA

**Whole Mount Fluorescent Staining of *Drosophila* Embryos**

Following dechorionization in 7.5% bleach, embryos from overnight collections were devitellinized and fixed in heptane with 4% formaldehyde in 0.3% PBT buffer (1x PBS with 0.3% Triton) for 25 min. Dechorionisation and dehydration was accomplished by vortexing and washing in methanol. Primary antibodies used: anti-ßGal (mouse 1:1000; Cappel), anti-Tin (rabbit 1:800; R. Bodmer). The secondary antibodies used were donkey anti-mouse-Alexa488 and anti-rabbit-Alexa568 (1:500, Molecular Probes). Flat preparations of embryos were mounted in Vectashield mounting medium and 70% glycerol (1:1). Stained embryos were examined under a confocal microscope (Zeiss LSM510) and images were processed using Adobe Photoshop.

**Identification of Mouse and Human Orthologs**

To identify orthologs between *Drosophila* and mouse and between *Drosophila* and human, we used pre-computed orthology predictions obtained from compara49, inparanoid, inparanoid6.1, inparanoid6.1 to ensembl, homologen08, and orthomclv2 (Kuzniar et al., 2008) databases. One-to-one and one-to-many mappings were observed between the *Drosophila* and the mammalian genes. In case of one–to–many mappings, all the ortholog targets for a given gene were considered for downstream analysis.

**Functional Annotation of "Heart Function" Hits**

Of the 490 RNAi hits (498 genes) with potential defects in heart function, we could annotate 377 genes by GO terms. To annotate the remaining 121 genes, we searched Panther db (http://www.pantherdb.org/). We were able to annotate an additional 116 genes with previously unknown functions.

**Gene Ontology (GO) Classification and Gene Set Enrichment**

GO analysis was performed using GOstat (http://gostat.wehi.edu.au/). GO analysis was run with *Drosophila* genes (and mouse or human orthologs) whose RNAi hits had a Z-score > 3. Over and under-represented ($p < 0.1$) GO terms with corrections for multiple testing (Yekutieli correction), were identified in the above list, compared to the FlyBase (fb) for *Drosophila*, Mouse Genome Informatics (mgi) for mouse and goa_human for human genes, respectively. Since terms that occur at a deeper level in the GO tree hierarchy and contain lesser number of genes are considered more biologically informative, we discarded terms containing more than 500 genes from further analysis. Significant GO terms were manually curated, pooled and organized into "functional groups," for visual representation of the GO data. A complete list of significantly enriched GO terms pooled into functional groups is provided in Table S4.

To remove any artificial bias in the gene list created by the ad hoc Z-score cut-off (>3) that we used previously in the GO analysis, we performed the Gene Set Analysis (GSA) to confirm enrichment of selected GO terms. GSA uses the entire list of genes corresponding to the selected biological terms and assesses if the process as a whole has been significantly altered in the entire dataset. A null hypothesis is that "Genes of a functionally irrelevant pathway are not clustered at the top of a rank ordered (based on Z-score) list of all genes in the experiment." Based upon the Z-score of the RNAi hit phenotype, a rank order list of 6892 unique genes corresponding to 8291 (with reported Z-score) RNAi transformants was created. Individual gene lists were constructed corresponding to 45 GO terms rendered significant by GO analysis (corrected $p < 0.1$). An enrichment score (Es) for a gene list (s) was calculated based upon the "heart function" Z-score using the formula:

Es = (Sum of average z-scores of all genes in s) / $\sqrt{}$ (Number of genes in s).

For every **s**, 100 bootstrap permutations were carried out to generate random functionally unrelated gene lists of the same size and their enrichment scores calculated as Er. A gene set s is considered enriched when Es > Er (90th quantile) and we reject the null hypothesis (p-value < 0.1). Enrichment of the GO term is also reported at p-value < 0.05 and 0.01.

**Pathway Analyses**

Pathway analysis was performed using the *Drosophila* Pathway database in GeneSpring GX. Briefly, the Pathway database in GeneSpring GX contains molecular relations from two sources: (1) those reported in open-source public databases like BIND and IntAct

(IMEX consortium) or (2) extracted from PubMed abstracts using a proprietary natural language processing technique. The tool UI allows a query of the database to build networks of molecular relations (edges) among molecules (nodes) of interest. Relations are classified as binding, expression, transport, protein modification, general regulation, metabolism and promoter binding. We constructed a network of "heart function" genes along with their first degree protein-protein interaction neighbors. Using filters in GeneSpring GX, we selected molecular relations reported by the IMEX consortium which represent "binding" interactions between the molecules. These interactions found the majority of binding partners for the heart hits. We also included the highest quality (Quality score $\geq$ 9) expression and promoter binding interactions using appropriate filter settings in GeneSpring GX. These interactions were manually curated and included in the final network.

**Pathway Enrichment Analysis**

A hypergeometric test, similar to the test used for GO enrichment analysis, was used to identify over-represented gene lists (C2 from Msigdb, BROAD Institute) and pathways (KEGG) among the "heart" hits. The hypergeometric test considers only the percentage representation of genes corresponding to a biological pathway in the pre-computed heart function gene list. This analysis was performed on the gene list identified as adult "heart" hits (Z-score $\geq$ 3) in *Drosophila* and their corresponding mouse or human orthologs, respectively.

**Pathway Systems Map**

For the combined systems map, all significant KEGG pathways and C2 gene sets were manually grouped into uniform functional categories as shown in Table S4, parts E–H. For uniformity, both lists have been manually annotated by the same functional classification terms. Functional classifications were assigned relevant to the biology of heart functions. For the systems map, we included all the functional categories assigned to the significant KEGG pathways. The information obtained from KEGG pathway analysis was supplemented with significant C2 gene sets from the appropriate functional categories: AKT/PI3K signaling activation, Calcium Signaling, cAMP regulated signaling, Cardiac related disease/signaling, Cytoskeleton, Hematopoeisis related, Ion Channels, muscle contraction, NFAT transcription, PI3K signaling, Txn factors. For each functional category, the corresponding genes that mapped to the KEGG pathways or C2 gene set were extracted. *Drosophila* orthologs for these genes were found and assigned to the respective pathway in the visual representation of the systems map. For the *Drosophila* systems map, *Drosophila* pathways that were over 90% enriched were manually annotated into functional groups. Corresponding heart hit genes and their first degree binding partners that overlapped with the gene set of the pathway were extracted and assigned to each pathway node in the systems map. We found both primary heart hits as well as binding partners filtered into the systems map are significantly enriched ($p < 0.01$) in cardiac genes of known function from independent studies, compared to any random list of the same size. We observe an almost equal enrichment of cardiac genes with known functions among the RNAi hits as well as binding partners included in the systems map.

**Generation of *not3* Knockout Mice**

For gene targeting of *not3* in mice, a targeting vector was constructed to replace exons 2 and 9 of the murine *not3* gene. The linearized construct was electroporated into A9 embryonic stem (ES) cells derived from 129/Ola and C57BL/6J hybrids. Approximately 2-3 in 100 ES cell clones were identified as correctly targeted by genomic Southern blotting. Chimeric mice from two independent clones transmitted the mutant allele through the germ line, and the targeted allele was confirmed by Southern blot. F1 mice were backcrossed for 5 times onto a C57BL/6 background. F5-F7 intercrossed mice were used for all experiments reported in this study. Mice were genotyped by PCR and Southern blotting and maintained at the animal facilities of the Institute of Molecular Biotechnology (IMBA), Akita University Graduate School of Medicine and Tokyo Medical and Dental University. All animal experiments were performed in accordance with institutional guidelines.

**Mouse Embryo Analyses**

To analyze blastocyst-stage mouse emryos, embryos at 3.5 dpc were flushed out from the uteri of pregnant mice of heterozygous x heterozygous breeding. RNA and Genomic DNA were extracted from individual blastocysts with Trizol (Invitrogen). Genotypes were determined by nested PCR, and reverse transcription was performed with Primescript RT reagent kit (TAKARA) followed by RT-PCR with ExTaq PCR kit (TAKARA). For immunohistochemistry of whole embryos, blastocysts were fixed in 4% PFA for 20 min, permealized with 0.4% Triton X-100 in PBS for 20 min, and blocked with 0.1% Triton X-100, 1% BSA or 10% donkey serum in PBS for 30 min. After each step embryos were washed five times for 5 min in PBS, and anti-Not3 antibody (Protein Tech Group, 11135-1-AP) staining was performed at 4°C overnight followed by Alexa543 secondary antibody for 1 hr. Embryos were mounted with VECTASHIELD with DAPI (Vector Labs) and observed under LSM500 confocal microscopy (Carl Zeiss). Embryos were collected and genotyped by nested PCR. For in vitro culture of inner cell mass outgrowth, blastocysts were individually cultured onto gelatinized tissue culture plates (Nunc) in standard ES medium with leukemia inhibitory factor (Chemicon) and photographed every few days. After cultivation, embryos were harvested by trypsinization and genotyped by PCR.

**mRNA and Protein Expression Analyses in Mice**

For real-time PCR analysis of mouse *not3*, 3 μg of DNase-treated total RNA was extracted from hearts and reverse transcribed using First-Strand Beads (GE Healthcare) with random primers. SYBR green real-time PCR reactions were carried out in 96-well plates

using an iQ-Cycler (Bio-Rad). Immunohistochemistry to detect *not3* was carried out with antibodies to NOT3 (Abcam 55681). Blastocysts were then counterstained DAPI.

The primer sets were as follows:

*Not3*-F: GTATAGCAAGGAGGGTCTGGGTCTGGCTCAG
*Not3*-R: TCGGGGTCCTGGGATGAGTCAACGTAGTAC
*ANF*-F: GAGAGACGGCAGTGCTTCTAGGC
*ANF*-R: CGTGACACACCACAAGGGCTTAGG
*βMyhc*-F: GACGAGGCAGAGCAGATCGC
*βMyhc*-R: GGGCTTCACAGGCATCCTTAGGG
*Kcnq1*-F: ATCAGGCGCATGCAGTACTTTG
*Kcnq1*-R: TGACATCTCGCACGTCGTAGG
*Kcne1*-F: TAGTGAATGTCGCCTTGTTTGGAA
*Kcne1*-R: TGGCATCTCACGGTGCTCTC
*Oct4*-F: CCAATCAGCTTGGGCTAGAG
*Oct4*-R: TGTCTACCTCCCTTGCCTTG
*GATA6*-F: GAGCTGGTGCTACCAAGAGG
*GATA6*-R: TGCAAAAGCCCATCTCTTCT
*Eomesodermin*-F: GGCAAAGCGGACAATAACAT
*Eomesodermin*-R: GACCTCCAGGGACAATCTGA
*18S*-F: CTGCCGTCTGAGTGTATCGC
*18S*-R: GCTGGGGCTGAGGAAAGTG
*GAPDH*-F: GGCCAAGGTCATCCATGACAAC
*GAPDH*-R: GTTGTCATGGATGACCTTGGCC

**Echocardiography**

Echocardiographic measurements were performed as described previously (Kuba et al., 2007). Briefly, mice were anesthetized with isoflurane(1%)/oxygen, and echocardiography was performed using an Acuson Sequoia C256 equipped with a 15-MHz linear transducer. Fractional shortening (FS) was calculated as follows: FS = [(LVEDD – LVESD)/LVEDD] x 100.

**Langendorff Perfusion Experiments**

*not3* heterozygous and littermate control mice were anaesthetized with ketamine/xylazine and isolated hearts immediately placed in cold PBS. The isolated heart was mounted on a Langendorff apparatus and perfused at a constant hydrostatic pressure of 75 mm Hg with an oxygenated Tyrode solution (37°C) composed of 136.9 mM NaCl, 5.4 mM KCl, 1.8 mM $CaCl_2$, 0.5 mM $MgCl_2$, 0.33 mM $NaH_2PO_4$, 10.0 mM glucose, and 5.0 mM HEPES as described (Murakami et al., 2007). Atropine (5.5 μM) was added to the perfusate, and a fluid-filled balloon catheter connected to a pressure transducer (CD200; NihonKoden) was inserted into the left ventricle via the left atrium. The sinoatrial node region was removed, and the heart was paced electrically at 400 beats/min (bpm). The electrical field stimulation (EFS) was applied in conjunction with the pacing stimulation (delay, 4 ms; duration, 1 ms for 5 s). Isoproterenol was perfused for 30 s using the indicated doses.

**Transverse Aorta Constriction (TAC)**

Eight to ten weeks old control wild-type littermates and *not3* heterozygous mice were subjected to pressure overload by TAC through constriction of the thoracic aorta as described (Kuba et al., 2007). Heart function was determined by echocardiography. For histology, hearts were arrested with 1 M KCl, fixed with 10% formalin, and embedded in paraffin. 5 μm thick sections were then cut and stained with hematoxylin and eosin (H&E). For detection of fibrotic areas, sections were stained with Masson-Trichrome.

**Treatment with HDAC Inhibitors**

For baseline measurements, wild-type and $not3^{+/-}$ mice were treated with vehicle, Trichostatin A (TSA) (Sigma, 0.6 mg/kg/day, i.p.), or Valproic acid (VPA) (Na Valproate (WAKO) 0.71% w/v in drinking water) for 1 week. For TAC heart failure experiments, the mice were given vehicle or VPA (0.71% w/v in drinking water) for 6 weeks starting one day after TAC or sham surgery.

**Western Blot Analysis for Histone Tail Modifications**

Acid-extracted histones were prepared from whole ventricles of mouse hearts as described (Cheung et al., 2000). Histones were resolved by SDS-PAGE (15%; 30:0.8) gels and transferred to nitrocellulose membranes for Western blotting. The amount of histone H3 was precalibrated with ponceau-S (Sigma) staining. Covalent modification status of H3 tails was analyzed using antibodies detecting acetylated H3K9 (Upstate), trimethylated H3K4 (Abcam), and anti-trimethylated H3K27 (kind gift from T. Jenuwein). Band intensities were quantified and normalized to total H3 levels.

### Human QT Interval Association

Human QT interval association signals over the *NOT3* region (official gene name *CNOT3*) were obtained from data generated by the QTSCD Consortium as described in (Pfeufer et al., 2009).

### Statistical Analyses

Data are presented as mean values ± SEM and were analyzed for differences between wild-type and *not3* heterozygous mice at discrete time points. *Drosophila* survival and heart function was analyzed by t test for single comparisons and ANOVA for multiple comparisons. Gene set enrichment is described above. GO enrichment was calculated using the online tool GOstat (http://gostat.wehi.edu.au/). For mouse heart function, normally distributed data were analyzed by t test. Data not normally distributed were analyzed using the Mann-Whitney test. $p < 0.05$ was considered significant. GWAS association results are presented as mean values ± SD.

#### SUPPLEMENTAL REFERENCES


Akasaka, T., Klinedinst, S., Ocorr, K., Bustamante, E.L., Kim, S.K., and Bodmer, R. (2006). The ATP-sensitive potassium (KATP) channel-encoded dSUR gene is required for Drosophila heart function and is regulated by tinman. Proc. Natl. Acad. Sci. USA *103*, 11999–12004.

Alayari, N.N., Vogler, G., Taghli-Lamallem, O., Ocorr, K., Bodmer, R., and Cammarato, A. (2009). Fluorescent Labeling of *Drosophila* Heart Structures. J. Vis. Exp. 10.3791/1423.

Cammarato, A., Dambacher, C.M., Knowles, A.F., Kronert, W.A., Bodmer, R., Ocorr, K., and Bernstein, S.I. (2008). Myosin transducer mutations differentially affect motor function, myofibril structure, and the performance of skeletal and cardiac muscles. Mol. Biol. Cell *19*, 553–562.

Cheung, P., Tanner, K.G., Cheung, W.L., Sassone-Corsi, P., Denu, J.M., and Allis, C.D. (2000). Synergistic coupling of histone H3 phosphorylation and acetylation in response to epidermal growth factor stimulation. Mol. Cell *5*, 905–915.

Dietzl, G., Chen, D., Schnorrer, F., Su, K.C., Barinova, Y., Fellner, M., Gasser, B., Kinsey, K., Oppel, S., Scheiblauer, S., et al. (2007). A genome-wide transgenic RNAi library for conditional gene inactivation in Drosophila. Nature *448*, 151–156.

Fink, M., Callol-Massot, C., Chu, A., Ruiz-Lozano, P., Izpisua Belmonte, J.C., Giles, W., Bodmer, R., and Ocorr, K. (2009). A new method for detection and quantification of heartbeat parameters in Drosophila, zebrafish, and embryonic mouse hearts. Biotechniques *46*, 101–113.

Han, Z., and Olson, E.N. (2005). Hand is a direct target of Tinman and GATA factors during Drosophila cardiogenesis and hematopoiesis. Development *132*, 3525–3536.

Kuba, K., Zhang, L., Imai, Y., Arab, S., Chen, M., Maekawa, Y., Leschnik, M., Leibbrandt, A., Markovic, M., Makovic, M., et al. (2007). Impaired heart contractility in Apelin gene-deficient mice associated with aging and pressure overload. Circ. Res. *101*, e32–e42.

Kuzniar, A., van Ham, R.C., Pongor, S., and Leunissen, J.A. (2008). The quest for orthologs: finding the corresponding gene across genomes. Trends Genet. *24*, 539–551.

Lo, P.C., and Frasch, M. (2001). A role for the COUP-TF-related gene seven-up in the diversification of cardioblast identities in the dorsal vessel of Drosophila. Mech. Dev. *104*, 49–60.

Murakami, M., Ohba, T., Wu, T.W., Fujisawa, S., Suzuki, T., Takahashi, Y., Takahashi, E., Watanabe, H., Miyoshi, I., Ono, K., et al. (2007). Modified sympathetic regulation in N-type calcium channel null-mouse. Biochem. Biophys. Res. Commun. *354*, 1016–1020.

Ocorr, K., Reeves, N.L., Wessells, R.J., Fink, M., Chen, H.S., Akasaka, T., Yasuda, S., Metzger, J.M., Giles, W., Posakony, J.W., and Bodmer, R. (2007). KCNQ potassium channel mutations cause cardiac arrhythmias in Drosophila that mimic the effects of aging. Proc. Natl. Acad. Sci. USA *104*, 3943–3948.

Paternostro, G., Vignola, C., Bartsch, D.U., Omens, J.H., McCulloch, A.D., and Reed, J.C. (2001). Age-associated cardiac dysfunction in *Drosophila melanogaster*. Circ. Res. *88*, 1053–1058.

Pfeufer, A., Sanna, S., Arking, D.E., MÜller, M., Gateva, V., Fuchsberger, C., Ehret, G.B., Orrú, M., Pattaro, C., Köttgen, A., et al. (2009). Common variants at ten loci modulate the QT interval duration in the QTSCD Study. Nat. Genet. *41*, 407–414.

Wolf, M.J., Amrein, H., Izatt, J.A., Choma, M.A., Reedy, M.C., and Rockman, H.A. (2006). Drosophila as a model for the identification of genes causing adult human heart disease. Proc. Natl. Acad. Sci. USA *103*, 1394–1399.

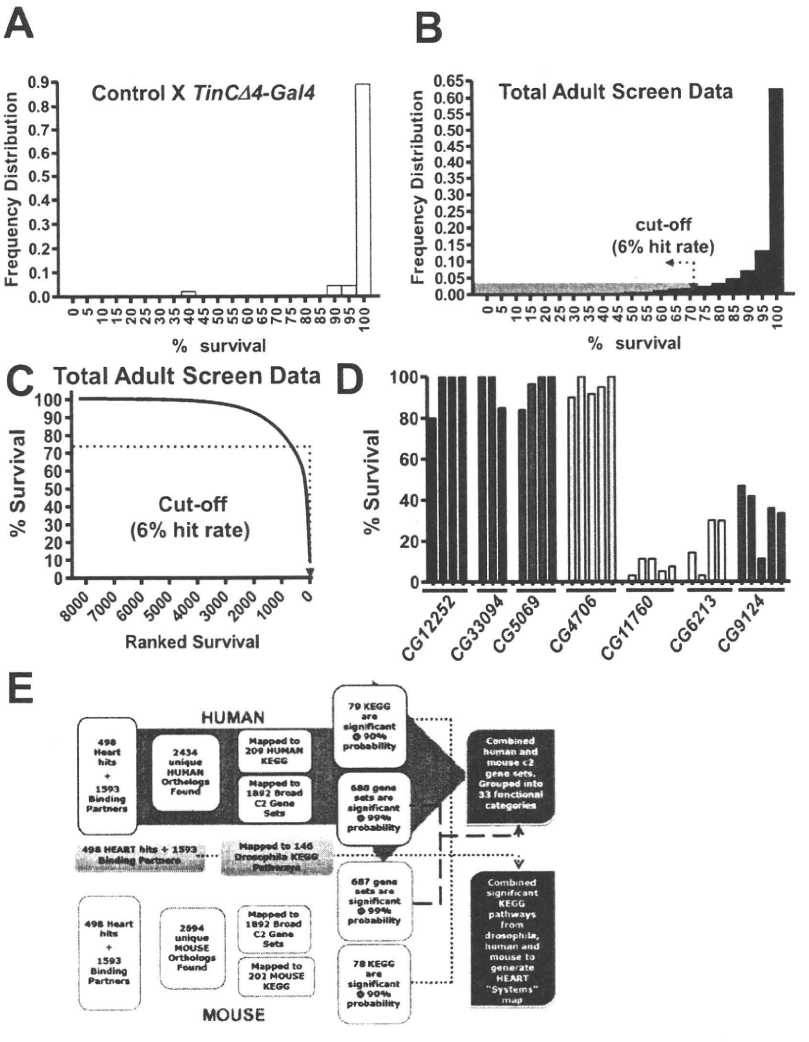


**Figure S1. Screen Set-up, Related to Figure 1**

(A) Repeated testing of our background control ($w^{1118}$) X heart driver (*TinCΔ4-Gal4*) line on multiple days shows a consistent ability of these flies to pass the increased ambient temperature. The *x* axis shows percent survival and the *y* axis the frequency of flies that passed (survival) or failed (death) the experimental challenge. n = 966 flies.

(B) Histogram for the entire heart screen shows the distribution of survival for all tested *TinCΔ4-Gal4*_RNAi lines. The cut-off used for *TinCΔ4-Gal4*_RNAi lines to pass the threshold for further analyses is indicated (Z-score > 3 corresponding to 72% survival). The *x* axis shows percent survival and the *y* axis the frequency of flies that passed (survival) or failed (death) the experimental challenge.

(C) Ranked Best Fit curve for the entire screen data set. The cut-off used for *TinCΔ4-Gal4*_RNAi lines to be included into our data-set for further analyses is indicated (Z-score > 3 corresponding to 72% survival.

(D) Representative repeat experiments for select *TinCΔ4-Gal4*_RNAi lines that passed or failed (recorded as % survival on day 6 after a shift to 29°C) to show reproducibility of the experimental model. Bar represent individual experiments for each RNAi line.

(E) Flow chart indicating KEGG and C2 gene set analysis in *Drosophila*, mice, and humans. Data from all three organisms were pooled to generate a global network map. See the Experimental Procedures for details.

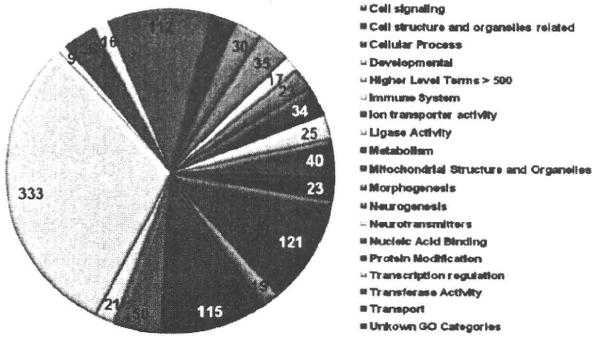


**Figure S2. *Drosophila* GO and KEGG Analysis, Related to Figure 2**

Functional classification of statistically enriched GO (gene ontology) terms for adult heart hits in *Drosophila*. Numbers indicate gene counts from all the GO terms included in each functional category. See Suppl. Table S4A contains the entire list of enriched GO terms and their classification into functional categories.

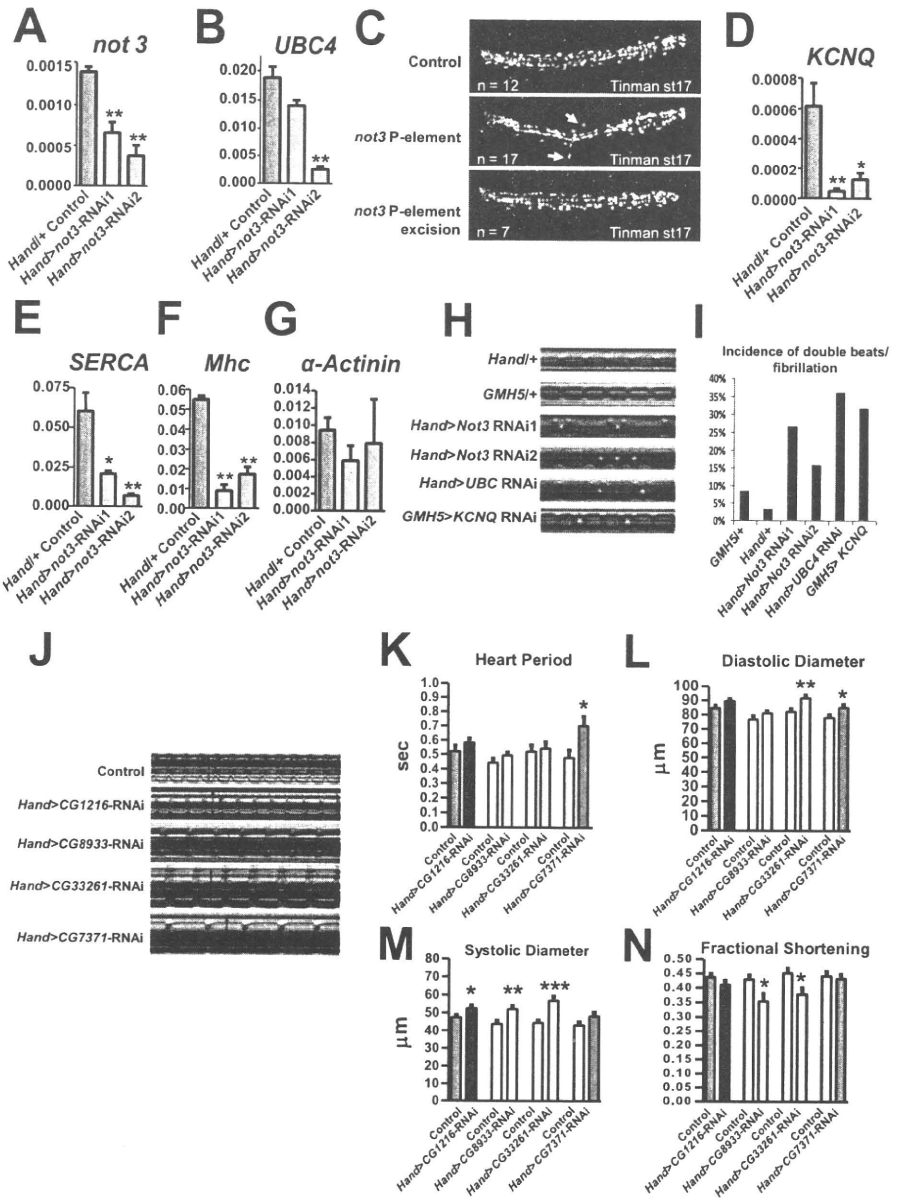


**Figure S3. Functional Phenotyping of Not3 and Other Candidate Heart Genes, Related to Figure 3**

(A and B) Expression levels of (A) *not3* and (B) *UBC4* in *Not3*-knockdown hearts.

(C) Wild-type embryonic heart at stage 17 (st17) stained with an anti-Tinman antibody (Tin). Four cell rows can be identified: two inner cardioblast cell rows and two outer pericardial cell rows. In *not3* mutants (P element; $CG8426^{KG10496}$) the inner cardioblast cell row is normal, whereas the pericardial cells are misarranged (arrows). Excision of the P-element completely rescues the phenotype observed in the *not3* mutant.

(D–G) Expression levels of (D) *KCNQ*, (E) *SERCA* (Calcium ATPase), (F) myosin heavy chain (*Mhc*) and (G) *α-Actinin* in *Not3*-knockdown hearts. mRNA transcripts were determined in 1-week-old adult fly hearts. 30 fly hearts were used for each sample. For statistical analysis, differences in mean values were calculated between $w^{1118}$ x *Hand-Gal4* control and each *Not3*-RNAi line. Mean values ± SEM are shown for each group. Student t test: * = $p < 0.05$, ** = $p < 0.01$.

(H) Heart specific knockdown of gene products in the Not3 complex results in an increase in the incidence of heart arrhythmia in one week old flies. M-modes made from movies of semi-intact fly heart preparations were examined for the presence of indications of developing arrhythmias (double beats and/or fibrillation episodes). M-modes from individual flies (4 s) with examples of these heartbeat irregularities (asterisks) are shown for heart-specific *Not3*, *UBC4*, and *KCNQ* knockdown using *Hand–Gal4* or *GMH5-Gal4* (Wessells et al., 2004).

(I) Quantification of fly heart records exhibiting one or more double beats and/or fibrillation episodes in a 30 s M-mode per fly is presented as a percent of the total number of flies (indicated in parentheses). Heart-specific knockdown of Not3 components results in an increased incidence of these irregularities compared to

control flies (*GMH5/+* and *Hand/+*). Because the total number of these irregular beats is relatively small they do not have a large effect on the overall arrhythmia index. However, the pattern of these irregularities (G) and the percentage of flies that exhibit them (H) is similar to what is seen in response to heart-specific knock-down of the *KCNQ* $K^+$ channel at one week (*GMH5>KCNQ* RNAi) that reflects what has been reported previously for one week old *KCNQ* mutant flies (Ocorr et al., 2007).

(J) M-modes reveal perturbations in normal wall movements induced by knock-down of the gene candidates *CG1216*, *CG8933*, *CG33261* and *CG7371*. Distance is measured in the y- and time is measured in the x-direction. Note the differences in heart wall diameters (double-headed red arrows), the extent of wall movement and the heart periods (the amount of time required for a complete contraction and relaxation cycle) relative to those of the control heart.

(K–N) The consequences of RNAi- mediated knockdown of *CG1216*, *CG8933*, *CG33261* and *CG7371* on cardiac dimensions and function. Knockdown of each gene appears to have a unique effect on overall cardiac performance since each line, relative to its control, exhibits a unique abnormal physiological signature. Unpaired t tests were performed to compare each *Hand-Gal4>UAS*-RNAi line to the corresponding $w^{1118}$ X *UAS*-RNAi control line.

Mean values ± SEM are shown for each group (n = 14 - 35). $^*p < 0.05$, $^{**}p < 0.01$, $^{***}p < 0.001$.

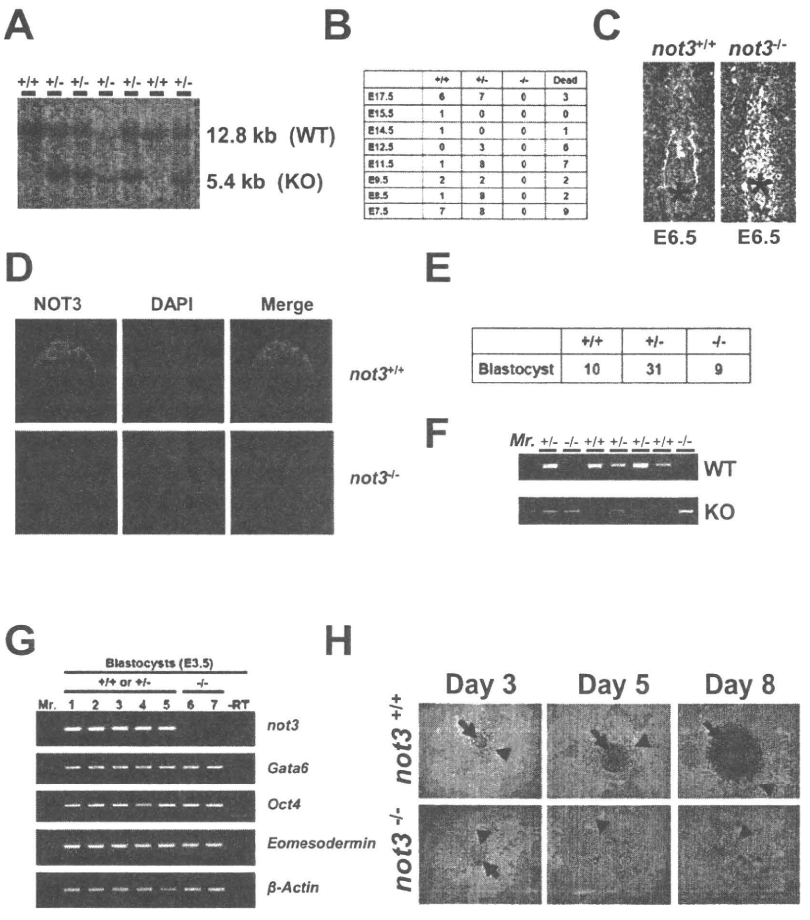


| | +/+ | +/- | -/- | Dead |
|---|---|---|---|---|
| E17.5 | 6 | 7 | 0 | 3 |
| E15.5 | 1 | 0 | 0 | 0 |
| E14.5 | 1 | 0 | 0 | 1 |
| E12.5 | 0 | 3 | 0 | 6 |
| E11.5 | 1 | 8 | 0 | 7 |
| E9.5 | 2 | 2 | 0 | 2 |
| E8.5 | 1 | 9 | 0 | 2 |
| E7.5 | 7 | 8 | 0 | 9 |

| | +/+ | +/- | -/- |
|---|---|---|---|
| Blastocyst | 10 | 31 | 9 |

**Figure S4. Generation and Embryology of *not3* Mutant Mice, Related to Figure 5**

(A) Southern Blot analyses for genomic DNAs of born off-spring from *not3* heterozygous matings. No homozygous null mice were obtained.

(B) Genotypes of embryos from *not3* heterozygous intercrosses. No viable homozygous null embryos were obtained at the indicated embryonic days (E) using timed pregnancies.

(C) Histological analysis of *not3*$^{-/-}$ mouse embryos. Longitudinal sections of E6.5 embryos in deciduas (asterix) are shown for wild-type and *not3*$^{-/-}$ embryos. H&E staining.

(D) Immunohistochemistry of NOT3 (red) in E3.5 wild-type (top) and *not3*$^{-/-}$ (bottom) blastocyst-stage embryos. Nuclei were counterstained using DAPI (blue). Note that Not3 localizes to nuclei and the cytoplasm.

(E) Frequency of *not3*$^{+/+}$, *not3*$^{+/-}$, and *not3*$^{-/-}$ E3.5 blastocysts from heterozygous intercrosses.

(F) Representative genotypes for blastocysts obtained from heterozygous intercrosses using PCR. Mr, molecular weight marker.

(G) RT-PCR analyses for mRNA expression of prototypic early embryonic marker genes. The epiblast marker genes *gata6* and *oct4* and the trophoblast marker *eomesodermin* appear to be normally expressed in *not3* null embryos.

(H) Blastocysts were recovered from heterozygous intercrosses, cultured individually, and genotyped by PCR. Cultures of representative wild-type and *not3*$^{-/-}$ epiblasts are shown for the indicated days. Arrows point at the ICM (inner cell mass). Arrowheads indicate the trophoblast.

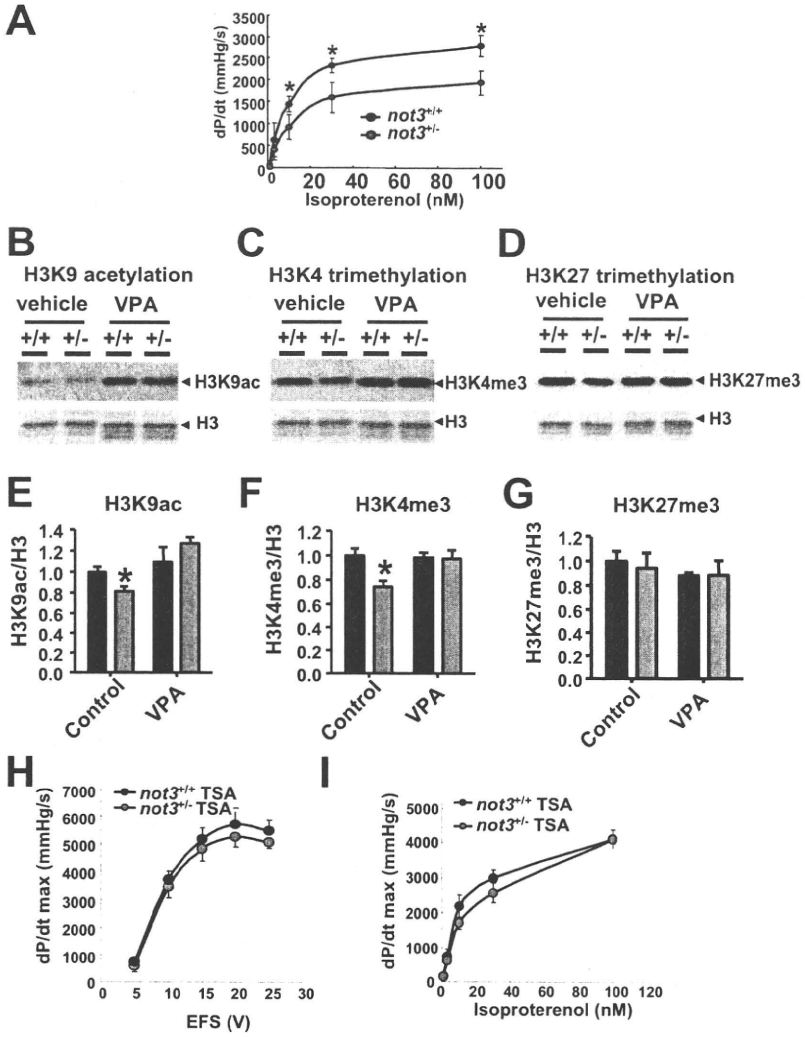


**Figure S5. Impaired Contractility and Histone Modifications in *Ex Vivo not3*$^{+/-}$ Mouse Hearts, Related to Figure 5**

(A) Left ventricular pressure (LVP) measurements in isolated *ex vivo not3*$^{+/-}$ and control *not3*$^{+/+}$ hearts under different doses of isoproterenol perfusion. *not3*$^{+/-}$ hearts from 4 months old mice showed impaired contractile responses to isoproterenol perfusion in the retrograde Langendorff mode as compared to age matched controls.

(B, E) H3K9 acetylation (H3K9ac) and (C, F) H3K4 trimethylation (H3K4me3) levels, but not (D, G) H3K27 trimethylation (H3K27me3) levels were decreased in *not3*$^{+/-}$ mouse hearts. Valproic acid (VPA) treatment reversed both (B, E) H3K9ac and (C, F) H3K4me3 levels of *not3*$^{+/-}$ hearts to those of littermate *not3*$^{+/+}$ hearts. Wild-type and *not3*$^{+/-}$ mice are treated with vehicle or VPA (0.71% w/v in drinking water) for 1 week, and histones were acid-extracted from whole heart ventricules. The histone extracts were separated by SDS-PAGE followed by immunoblotting with specific antibodies for each modified lysine residues of H3. Band intensities were quantified and normalized to total H3 levels. Representative immunoblot pictures (top) and corresponding ponceau S-stained membranes (bottom) are shown in (B-D), and the respective quantified levels of H3K9ac, H3K4me3 and H3K27me3 are shown in (E-G). n = 5-12 per group.

Treatment with the HDAC inhibitor Trichostatin A (TSA) reversed the impaired contractile response of *ex vivo not3*$^{+/-}$ hearts to (H) electrical field stimulation (EFS) or (I) isoproterenol perfusion to wild-type levels. Wild-type and *not3*$^{+/-}$ mice were treated with vehicle or TSA (0.6 mg/kg/day, *i.p.*) for 1 week. Hearts were then excised and subjected to Langendorff perfusion. Ex vivo heart contractility was assayed in response to different EFS stimulations or different doses of isoproterenol perfusion. No statistically significant differences were detected at any dosage/stimualtion points between *not3*$^{+/+}$ and *not3*$^{+/-}$ mice. n = 6-8 per group. All values are mean +/− SEM * $p < 0.05$.

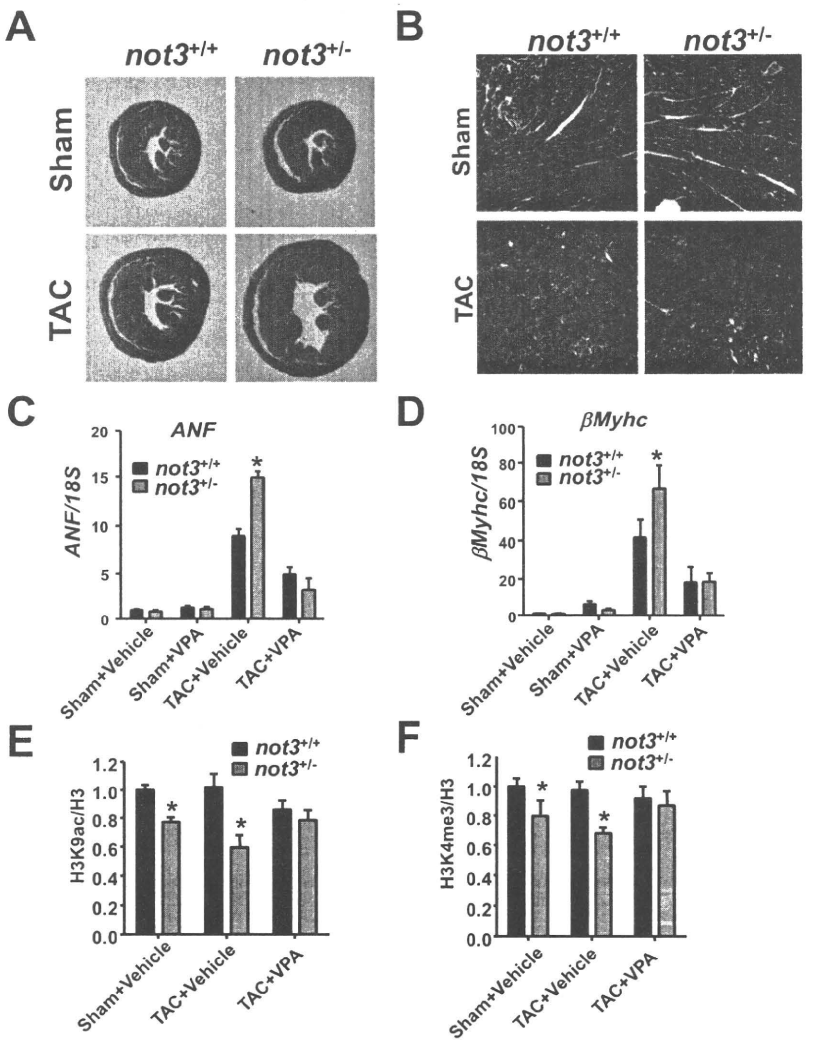


**Figure S6. Severe Cardiac Hypertrophy and Fibrosis in *not3*$^{+/-}$ Mice under Pressure Overload and Rescue of Disease Markers and Histone Modification by Treatment with VPA, Related to Figure 7**

Representative sections of *not3*$^{+/+}$ and *not3*$^{+/-}$ hearts analyzed 3 weeks after sham or transverse aortic constriction (TAC) surgery.

(A) Hematoxylin & eosin staining.

(B) Masson-trichrome staining to visualize collagen deposits indicative of fibrotic changes. Note cardiac hypertrophy and ventricular dilation in *not3*$^{+/-}$ mice following TAC.

(C and D) Real time PCR analyses for (C) *ANF* (atrial natriuretic factor) and (D) *βMyhc* (ß-myosin heavy chain) mRNA expression. Total RNA was isolated from hearts 6 weeks after TAC or sham surgery in the presence of vehicle or the HDAC inhibitor VPA. *ANF* and *βMyhc* levels were normalized to *18S* mRNA.

(E and F) In vivo administration of the HDAC inhibitor Valproic acid (VPA) restores (E) reduced H3K9 acetylation (H3K9ac) and (F) H3K4 trimethylation (H3K4me3) in post-TAC *not3*$^{+/-}$ mouse hearts to that of wild-type control levels. Wild-type and *not3*$^{+/-}$ mice were treated with vehicle or VPA (0.71% w/v in drinking water) for 6 weeks after TAC or sham surgery. Histones were acid-extracted from whole heart ventricules, separated by SDS-PAGE, and immunoblotted with antibodies specific to H3K9ac and H3K4me3. Band intensities were quantified and normalized to total H3 levels. All values are mean +/– SEM *; $p < 0.05$ n = 5-8 per group.